

Article

Control Strategy Optimization for Parallel Hybrid Electric Vehicles Using a Memetic Algorithm

Yu-Huei Cheng¹ and Ching-Ming Lai^{2,*}

¹ Department of Information and Communication Engineering, Chaoyang University of Technology, Taichung 41349, Taiwan; yuhuei.cheng@gmail.com

² Department of Vehicle Engineering, National Taipei University of Technology, 1, Sec. 3, Chung-Hsiao E. Road, Taipei 106, Taiwan

* Correspondence: pecmlai@gmail.com; Tel.: +886-2-2771-2171 (ext. 3612)

Academic Editor: Hongwen He

Received: 15 January 2017; Accepted: 1 March 2017; Published: 3 March 2017

Abstract: Hybrid electric vehicle (HEV) control strategy is a management approach for generating, using, and saving energy. Therefore, the optimal control strategy is the sticking point to effectively manage hybrid electric vehicles. In order to realize the optimal control strategy, we use a robust evolutionary computation method called a “memetic algorithm (MA)” to optimize the control parameters in parallel HEVs. The “local search” mechanism implemented in the MA greatly enhances its search capabilities. In the implementation of the method, the fitness function combines with the ADvanced VehIcle SimulatOR (ADVISOR) and is set up according to an electric assist control strategy (EACS) to minimize the fuel consumption (FC) and emissions (HC, CO, and NO_x) of the vehicle engine. At the same time, driving performance requirements are also considered in the method. Four different driving cycles, the new European driving cycle (NEDC), Federal Test Procedure (FTP), Economic Commission for Europe + Extra-Urban driving cycle (ECE + EUDC), and urban dynamometer driving schedule (UDDS) are carried out using the proposed method to find their respectively optimal control parameters. The results show that the proposed method effectively helps to reduce fuel consumption and emissions, as well as guarantee vehicle performance.

Keywords: hybrid electric vehicle (HEV); control strategy; memetic algorithm (MA); parameters optimization

1. Introduction

The development of clean vehicles with high fuel economy and low emissions is gradually becoming mainstream in the automotive industry owing to the aggravation of the global energy crisis and environmental problems. In the field of vehicle engineering, conventional power systems driven by internal combustion engines (ICEs) have several disadvantages that adversely affect fuel economy and emissions. Furthermore, ICEs are generally over-designed approximately 10 times to meet the required vehicle driving performance that causes the cruising operating point to deviate away from the optimal operation point [1]. Hybrid electric vehicles (HEVs) do not certainly require external battery charging and new infrastructure; therefore, many researchers have focused on HEV in the past few years. Additionally, their superior fuel economy and lower emissions with no compromise in dynamic performance make HEVs a viable solution for providing cleaner and more fuel-efficient vehicles. Tanoue et al. [2] pointed out that hybrid technology is of crucial importance for future automobiles.

An HEV includes at least two energy converters, i.e., ICE and an electric motor (EM), to generate the mechanical energy required to drive the vehicle and operate the on-board accessories. Therefore, energy flow management plays an important role in HEV efficiency. In order to make HEVs as efficient as possible, the HEV control strategy [3–11] is used to properly manage their energy components.

By designing an appropriate control strategy, the HEV not only cuts down toxic exhaust emissions, but also maintains the performance of the road-driven vehicle while minimizing fuel consumption. A parameter-optimized control strategy can be used to solve this problem.

In early studies, rule-based control was widely used for parametric optimization. Dynamic programming (DP) can be used to decide the global optimal control parameters [12] when the driving cycle and vehicle performance are known. Pontryagin's minimum principle (PMP) may be used to determine the local optimal control parameters, and it can obtain an optimal trajectory in less computing time than DP [13]. Many HEVs have been discussed in literature, Assanis et al. attempted to improve the fuel consumption (FC) while maintaining the driving performance within the standard limits and using the determined optimal sizes of the ICE, EM and battery pack [14]. Sciarretta et al. proposed equivalent consumption minimization strategy (ECMS) a strategy based on the definition of the fuel equivalent of the electrical energy for the real-time load control of parallel HEVs [15]. Johri and Filipi [16] developed a supervisory controller for HEVs based on the principles of reinforcement learning and neuro-dynamic programming to overcome the curse of dimensionality, and solving policy optimization for a system with very large design state space. Poursamad and Montazeri [17] presented a fuzzy logic controller that is tuned by a genetic algorithm for parallel HEVs to minimize fuel consumption and emissions. Panday and Bansal developed a fuel efficient energy management strategy which for power-split hybrid electric vehicle using modified state of charge estimation method. Their energy management strategy adapts GA to compute the optimal values of various governing parameters, and then uses Pontryagin's minimum principle to decide the threshold power at which engine is turned on [18]. Several targets are usually considered simultaneously in HEV control strategy. To minimize vehicle fuel consumption and engine emissions, and maintain driving performance is the primary purpose of an HEV control strategy. Control strategies designed based on engineering intuition usually fail to achieve satisfactory overall system efficiency owing to the complex nature of HEVs. Several studies based on evolutionary computation have been proposed to determine the optimal parameters for the control strategy for HEVs. Montazeri and Poursamad [19] proposed a genetic algorithm (GA) to minimize the weighted sum of FC and emissions, and they also considered the Partnership for a New Generation of Vehicles (PNGV) performance requirements as constraints [20]. Wu et al. [21] employed a particle swarm optimization (PSO) method to determine the optimal parameters of the powertrain and the control strategy to reduce the FC, emissions, and manufacturing costs of HEVs. Long and Nhan [22] used bees algorithm (BA) to minimize the weighted sum of FC and emissions, and considered the PNGV constraints for the vehicle performance. Hao et al. [23] employed the DIvided RECTangle (DIRECT) algorithm to optimize the extracted seven key parameters based on the optimization model of the key parameters from the perspective of fuel economy. More other control algorithms for HEVs can be referred to [24,25].

The characteristics of the powertrain system are highly non-linear and discontinuous, and may contain several local optima. However, many methods proposed in the literature lack local search capabilities that makes the optimal solution is difficult to obtain. In this study, a robust evolutionary computation method—memetic algorithm (MA) [26] is proposed to optimize the control parameters. The "local search" mechanism implemented in the MA greatly enhances its search capabilities. Therefore, it is particularly suitable for solving such problems. MAs were inspired by Dawkins' notion of a meme [27]. They are similar, yet superior to the GA. MAs progress through a local search before becoming involved in the evolution process [28] to ensure that all chromosomes and offspring gain some experiences. To solve this problem, a single objective problem is used and a goal-attainment method is substituted for the original multi-objective optimization problem. The goal of optimization in this problem is to minimize the engine fuel consumption and emissions within the given criteria. In addition, vehicle performance requirements must also be maintained. The used fitness function is proposed according to an electric assist control strategy (EACS) [4]. The proposed method is then performed for four different driving cycles, including new European driving cycle (NEDC), Federal

Test Procedure (FTP), Economic Commission for Europe + Extra-Urban driving cycle (ECE + EUDC) and urban dynamometer driving schedule (UDDS).

Using MAs to solve the control strategy optimization problem associated with minimizing engine fuel consumption and emissions while maintaining driving performance saves a considerable amount of time and provides a global optimal solution. The MA proposed for the control strategy optimization correctly and quickly identifies the optimal parameters required for parallel HEVs. Our experimental results further indicate that MAs applied in the design of control strategy are effective in minimizing minimize fuel consumption and emissions while maintaining driving performance.

2. Configurations of HEVs

Before discussing the configurations of HEVs, we first mention the differences between a conventional HEV and a plug-in HEV. There are two fundamental differences between them, one is the main power source and the other is the whole energy efficiency of the two vehicle architectures. The main power source is a gasoline-powered ICE for conventional HEVs, while it is a battery-powered electric motor for plug-in HEVs. In conventional HEVs, the electric motor is used to complement the ICE and electricity is generated on board. Its energy savings are not substantial in comparison to plug-in HEVs. In plug-in HEVs, the ICE is used to complement the electric motor and grid-supplied electricity. Its energy savings are more substantial than conventional HEVs. Other types of prominent technology [29] are also used. Series and parallel type are currently two common configurations for HEVs. Another common type of HEV synthesizes the characteristics of both series and parallel types and is called dual-mode or multi-mode type [30].

2.1. Series HEV

The configuration of a series type HEV mainly consists of a fuel converter/ICE, a generator, an energy storage system/battery, and an electric motor, as shown in Figure 1. In the series HEV, the fuel converter does not directly drive the vehicle wheels. On the contrary, the series HEV uses a generator to convert mechanical power into electrical energy that is stored in the battery and to provide the electric motor power to achieve the torque required to drive the wheels.

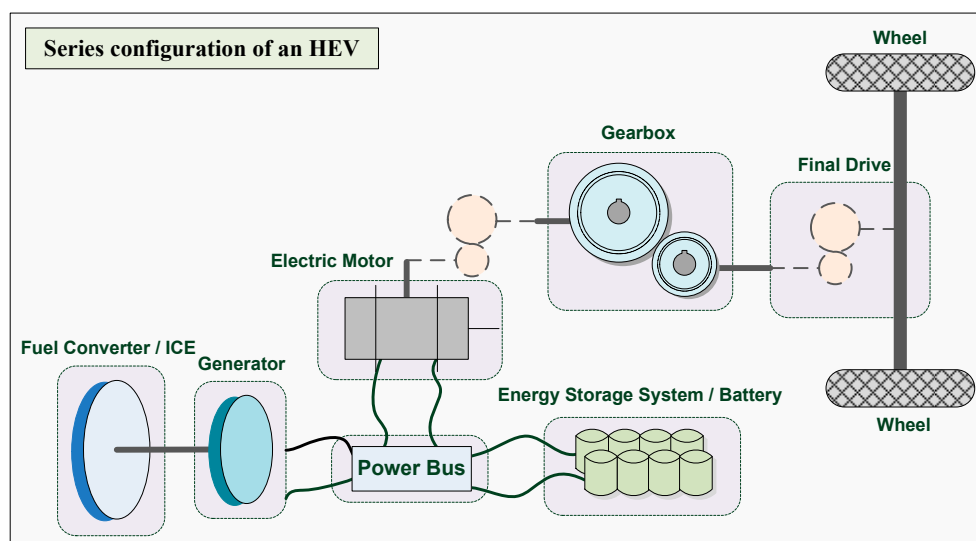


Figure 1. Series configuration of a hybrid electric vehicle (HEV).

2.2. Parallel HEV

In the configuration of a parallel type HEV, the fuel converter and the electric motor both transmit power to the vehicle, as shown in Figure 2. The electric motor can also be used as a generator to

charge the battery via the regenerative brake or by absorbing the excess power of the fuel converter. In comparisons, the parallel type is better than the series type in the configuration. The parallel type has a smaller fuel converter and a smaller electric motor than the series type while it provides the same performance. This characteristic makes the parallel type HEV more suitable for heavy-duty passenger vehicles than the series type.

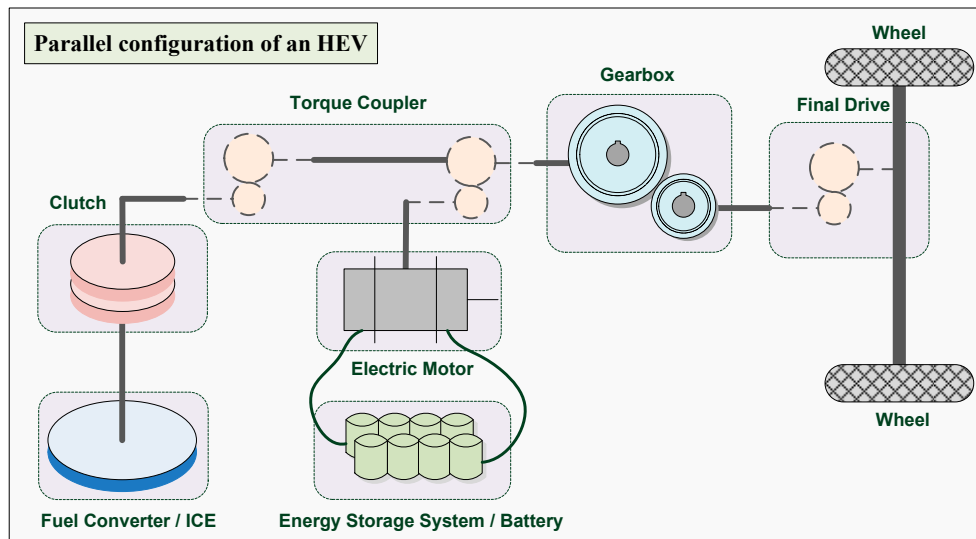


Figure 2. Parallel configuration of an HEV.

2.3. Dual-Mode HEV

The configuration of the synthesized series–parallel type includes additional mechanical links as compared to the configuration of the series type, and it has an additional generator as compared to the configuration of the parallel type. That makes the synthesized series–parallel type relatively more complex and expensive than the series and parallel types.

3. Control Strategy for Parallel HEV

There are two power-drive units (i.e., fuel converter and electric motor) integrated into the parallel type; therefore, the purpose of the control strategy of the parallel HEV is to decide how to allocate the required torque between the fuel converter and the electric motor during driving. When positive torque is requested, the summation of torques for the fuel converter and electric motor is equal to the demand of the driver. On the contrary, when negative torque is requested, the summation of torques for the electric motor and brake is equal to the demand of the driver while the engine torque is zero.

Several control strategies have been employed for parallel HEVs. EACS [4] is the most commonly used control strategy; the fuel converter is the major energy provider, and the electric motor is the assistant component for fuel converter. The baseline control strategy (BCS) is used by the ADvanced VehIcle SimulatOR (ADVISOR) in a parallel HEV. Eight independent input parameters are defined to minimize the engine energy usage, and the variables are also usually defined for an EACS [19], as listed in Table 1. This EACS is a common method of hybrid control; examples of its application are the Toyota Prius [31] and Honda Insight [32].

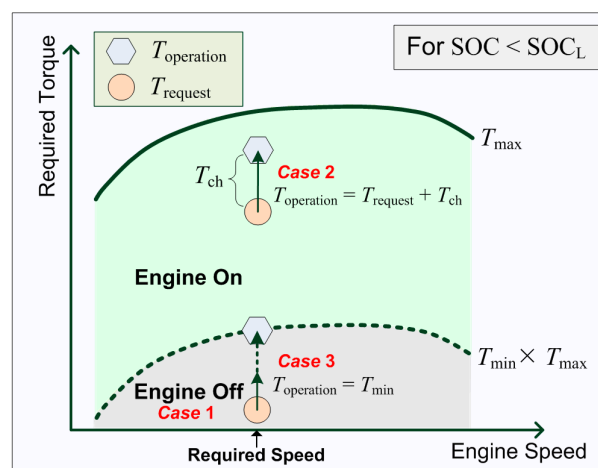
Table 1. Eight independent input parameters/variables for an electric assist control strategy (EACS).

Parameter	BCS Variable [8]	Description
SOC_L	cs_lo_soc	The lowest state of charge allowed.
SOC_H	cs_hi_soc	The highest state of charge allowed.
T_{ch}	cs_charge_trq	An alternator-like torque loading on the engine to recharge the battery pack.
T_{min}	cs_min_trq_frac	When commanded at a lower torque, the engine will be manipulated at the threshold torque (minimum torque threshold = $T_{min} \times T_{max}$). Additionally, if $SOC < SOC_L$, the electric motor serves as a generator.
T_{off}	cs_off_trq_frac	When commanded at a lower torque and if $SOC > SOC_L$, the engine will be shut down (minimum torque threshold = $T_{off} \times T_{max}$).
ELS_L	cs_electric_launch_spd_lo	The lowest vehicle speed threshold.
ELS_H	cs_electric_launch_spd_hi	The highest vehicle speed threshold.
D_{ch}	cs_charge_deplete_bool	To use charge deplete strategy or charge sustaining strategy.

The electric motor is used by the EACS in several specific ways:

- (1) When the battery state of charge (SOC) is more than SOC_L , the engine will be shut down if the required speed is less than the ELS , which is also called the electric launch speed (as shown in Figure 4, Case 1).
- (2) When the required torque is less than a minimum torque threshold ($T_{off} \times T_{max}$), the engine will also be shut down (as shown in Figure 4, Case 2).
- (3) The electric motor will provide the total required torque when the engine is shut down (as shown in Figure 4, Cases 1 and 2, and Figure 3, Case 1).
- (4) When the battery SOC is less than its SOC_L , an alternator-like torque (T_{ch}) is provided from the engine to charge the battery (as shown in Figure 3, Case 2). This alternator-like charging torque is proportional to the difference between the SOC and the average of the SOC_L and SOC_H .
- (5) The engine charging torque is only applied when the engine is started up (as shown in Figure 3, Case 2).
- (6) To avoid the engine working at an inefficient low torque status, the engine torque must be maintained at the minimum torque threshold ($T_{min} \times T_{max}$) (as shown in Figure 3, Case 3).

The fuel consumption, emissions, battery charge, and vehicle performance are greatly influenced by the control strategy parameters. Consequently, we proposed the robust evolutionary computation method MA to optimize the control parameters in this study.

**Figure 3.** EACS for low SOC.

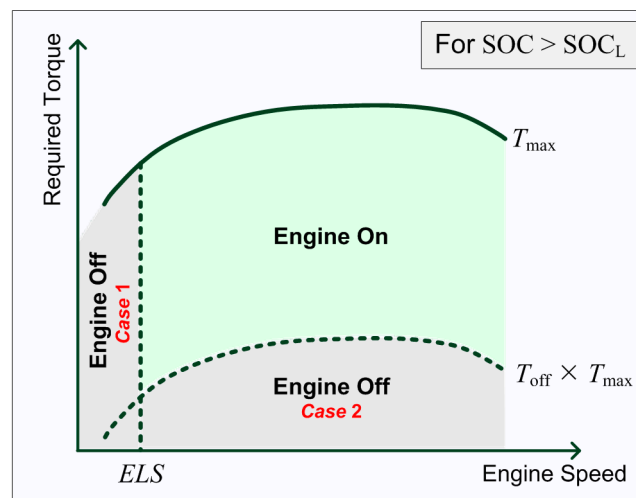


Figure 4. Electric assist control strategy (EACS) for high state of charge (SOC).

4. Definition of Objective Function

In the optimization of the control strategy parameters, there are two different approaches to be considered [33,34], and they have already been applied to all types of evolutionary computation-based methods related to this problem [19,21,22]. The two different approaches are to optimize a single objective function that is a weighted aggregation of some of the goals and to define the other goals as constraints. Several simultaneous goals including the FC, emissions, charge requirement, and driving performance are managed in the HEV control strategy. In the other words, the HEV control strategy must minimize the weighted sum of the FC and emissions (HC, CO and NO_x) while meeting the charge sustaining requirement and driving performance. We thus define FC, HC, CO, and NO_x as a single objective function that is a weighted aggregation as shown in Equation (1):

$$\text{Objective}(x) = (w_{fc} \times \text{FC}) + (w_{hc} \times \text{HC}) + (w_{co} \times \text{CO}) + (w_{nox} \times \text{NO}_x) \quad (1)$$

where x is a vector that consists of eight parameters of the control strategy as shown in above-mentioned Table 1. Chromosome encoding in Section 5. The design of MA for optimize control strategy of parallel HEVs in details); w_{fc} , w_{hc} , w_{co} , and w_{nox} are defined as weighting factors employed to respectively investigate the influences of the different objectives of FC, HC, CO, and NO_x on the optimization results.

Furthermore, we use the PNGV [20] as the dynamic performance requirements to guarantee that the vehicle performance is still maintained during optimization. Table 2 describes the seven PNGV dynamic performance constraints considered.

Table 2. The seven PNGV dynamic performance constraints considered [22]. PNGV: partnership for a new generation of vehicles.

Parameter	Description	y_i	$c_i(x)$
Acceleration time	Acceleration time 1 for 0–60 mph in 12 s	1.2	$c_1(x)$
	Acceleration time 2 for 40–60 mph in 5.3 s	1.5	$c_2(x)$
	Acceleration time 3 for 0–85 mph in 23.4 s	1.2	$c_3(x)$
Maximum speed	≥ 0.017 mi/s	1.2	$c_4(x)$
Maximum acceleration	≥ 0.0032 mi/s ²	1.2	$c_5(x)$
Distance in 5 s	≥ 0.0265 mi	1.2	$c_6(x)$
Gradeability	6.5% gradeability at 55 mph with 272 kg additional weight for 20 min	2.0	$c_7(x)$

In order to apply the MA directly to the constrained optimization problem, the seven PNGV constraints are integrated into the objective function [35] as shown in Equation (2):

$$\min_{x \in S} \text{Objective}(x) \text{ s.t. } c_i(x) \leq 0, i = 1, 2, 3, \dots, 6, 7 \quad (2)$$

where x is a vector of the parameters of the control strategy as mentioned above and it is a solution within the solution space S ; $\text{Objective}(x)$ is the objective function; and $c_i(x)$ is the PNGV dynamic performance constraints.

5. The Design of MA for Optimized Control Strategy of Parallel HEVs

MAs were inspired by Dawkins' conception [27,36]. The adjective 'memetic' is derived from the term 'meme', which denotes an analogue to a gene in the context of cultural evolution [26]. Similar to GAs, the evolutionary computations involved, such as selection, crossover and mutation are effective in implementing optimal solutions for the control strategy of parallel HEVs. However, in contrast to GAs, MAs progress through a local refinement of individuals before becoming involved in the evolution process and thus assure that all individuals and offspring gain some experiences. After each run, individuals in an MA share information with each other, and superior solutions based on a fitness rule are refined from generation to generation [37].

The flowchart of the proposed MA for the optimize control strategy is shown in Figure 5. There are eight dissociated procedures included: (1) chromosome encoding; (2) population initialization; (3) local search; (4) fitness evaluation; (5) ADVISOR evaluation; (6) judgment on termination conditions; (7) selection, crossover, and mutation processes; and (8) replacement process. These eight procedures are described below.

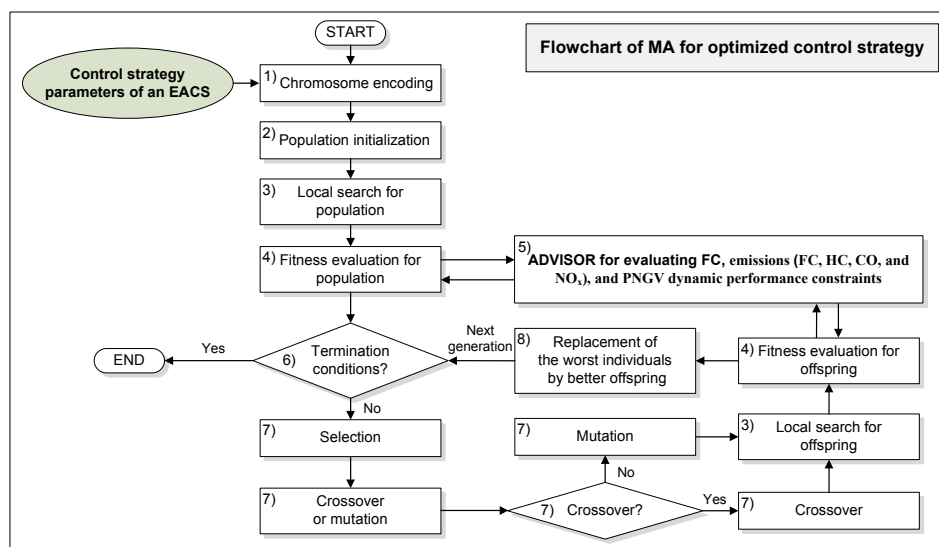


Figure 5. Flowchart of memetic algorithm (MA) for optimize control strategy.

(1) Chromosome encoding

In order to use the MA to optimize the control strategy parameters in parallel HEVs, a chromosome encoding x must first be defined. In this study, we use eight independent control strategy parameters of an EACS as shown in Table 1 as the chromosome encoding for this optimization problem. The chromosome encoding x is a vector with eight dimensions as shown in Equation (3):

$$x = (\text{SOC}_L, \text{SOC}_H, T_{ch}, T_{\min}, T_{\text{off}}, \text{ELS}_L, \text{ELS}_H, D_{ch}) \quad (3)$$

where x represents a vector that encodes eight parameters of the control strategy.

(2) Population initialization

When performing the MA algorithm for the control strategy optimization, at the start, dozens of chromosomes $x = (SOC_L, SOC_H, T_{ch}, T_{min}, T_{off}, ELS_L, ELS_H, D_{ch})$ are randomly generated for an initial population without duplicates. The values of $SOC_L, SOC_H, T_{ch}, T_{min}, T_{off}, ELS_L, ELS_H$ and D_{ch} are randomly generated between default bounds given by the EACS constraint. Their default bounds are presented in Table 3.

Table 3. Range of the parameters of the EACS constraints for the proposed method.

Parameter (Unit)	Lower Bound	Upper Bound
SOC_L (-)	0.1	0.5
SOC_H (-)	0.55	1
T_{ch} (Nm)	1	80.9
T_{min} (-)	0.05	1
T_{off} (-)	0.05	1
ELS_L (m/s)	0	15
ELS_H (m/s)	10	30
D_{ch} (-)	0	1

(3) Local search

The local search is the highly capable of identifying superior individuals (i.e., chromosomes with good fitness) from amongst the neighbors of an original individual. The experience of the original individual will be improved by getting experience from the neighbors, and thus a local optimum solution can be acquired. At the beginning of the algorithm, the local search process is performed by all individuals in order to acquire the local optimality of each individual. Furthermore, the local search process is also performed by new generated individuals in each iteration in order for the local optimum to always be retained. Finally, a global optimum is determined. We applied the pseudo-code of the local search to the proposed method which is as follows.

Local Search Pseudo-Code for the Proposed Method

```

1 Begin;
2   Select an incremental value  $d = a \times Rand()$ ;
3   For a given individual  $i \in Population$ : calculate fitness ( $i$ );
4   For  $j = 1$  to the number of variables in individual  $i$ ;
5     value ( $j$ ) = value ( $j$ ) +  $d$ ;
6     calculate fitness ( $i$ );
7     If fitness of the individual is not improved then
8       value ( $j$ ) = value ( $j$ ) -  $d$ ;
9     else if fitness of the individual is improved then
10      retain value ( $j$ );
11   Next  $j$ ;
12 End;
```

(4) Fitness evaluation

The fitness function is a function used to evaluate the fitness of the chromosomes in the individuals. To make use of the MA in the simultaneous optimization of parallel HEVs in the study, the fitness function adapts the inverse of the objective function $Objective(x)$ in Equation (1) and the seven PNGV dynamic performance constraints are considered as penalty functions to maximize the fitness value as shown in Equation (4):

$$fitness(x) = 1 / [Objective(x) + \sum_{i=1}^7 y_i \times p_i(x)] \quad (4)$$

where y_i are penalty factor selected by trial and error [22] as indicated in Table 2, and $p_i(x)$ are penalty functions that are related to the i -th constraint $c_i(x)$ in Table 2.

The seven penalty functions $p_i(x), i = 1, 2, 3, \dots, 6, 7$ for the PNGV dynamic performance constraints are respectively shown in the following Equations (5)–(11).

- Acceleration time 1

$$p_1(x) = \begin{cases} 0, & \text{if acceleration time 1 satisfied the PNGV acceleration time 1} \\ \text{acceleration time 1} - \text{PNGV acceleration time 1}, & \text{if acceleration time 1} > \text{PNGV acceleration time 1} \end{cases} \quad (5)$$

- Acceleration time 2

$$p_2(x) = \begin{cases} 0, & \text{if acceleration time 2 satisfied the PNGV acceleration time 2} \\ \text{acceleration time 2} - \text{PNGV acceleration time 2}, & \text{if acceleration time 2} > \text{PNGV acceleration time 2} \end{cases} \quad (6)$$

- Acceleration time 3

$$p_3(x) = \begin{cases} 0, & \text{if acceleration time 3 satisfied the PNGV acceleration time 3} \\ \text{acceleration time 3} - \text{PNGV acceleration time 3}, & \text{if acceleration time 3} > \text{PNGV acceleration time 3} \end{cases} \quad (7)$$

- Maximum speed

$$p_4(x) = \begin{cases} 0, & \text{if max speed satisfied the PNGV max speed} \\ \text{PNGV max speed} - \text{max speed}, & \text{if max speed} < \text{PNGV max speed} \end{cases} \quad (8)$$

- Maximum acceleration

$$p_5(x) = \begin{cases} 0, & \text{if max acceleration satisfied the PNGV max acceleration} \\ \text{PNGV max acceleration} - \text{max acceleration}, & \text{if max acceleration} < \text{PNGV max acceleration} \end{cases} \quad (9)$$

- Distance in 5 s

$$p_6(x) = \begin{cases} 0, & \text{if distance in 5 s satisfied the distance in 5 s} \\ \text{PNGV distance in 5 s} - \text{distance in 5 s}, & \text{if distance in 5 s} < \text{PNGV distance in 5 s} \end{cases} \quad (10)$$

- Gradeability

$$p_7(x) = \begin{cases} 0, & \text{if grade satisfied the PNGV ggrade} \\ \text{PNGV grade} - \text{grade}, & \text{if grade} < \text{PNGV grade} \end{cases} \quad (11)$$

(5) ADVISOR evaluation

ADVISO R is an abbreviation of “ADvanced VehIcle SimulatOR” which is written in the MATLAB/Simulink environment and was developed by the National Renewable Energy Laboratory in November 1994. It provides the vehicle engineering community with an easy-to-use, flexible, yet robust and supported analysis package for advanced vehicle modeling [38]. In order to effectively measure the FC, emissions (HC, CO, and NO_x), and driving performance for the used control strategy in parallel HEVs, we have combined the ADVISO R with the proposed MA to evaluate the fitness in chromosomes. When the fitness function is called, the control strategy variables will be passed on to the ADVISO R to calculate the FC, emissions (HC, CO, and NO_x), and driving performance and return their values. These values will then be used to evaluate the fitness of the control strategy.

(6) Judgment on termination conditions

The termination conditions provide the evolutionary computation method to stop meaningless and endless computations. Here, two termination conditions are employed in the proposed method. One is that the maximum number of iterations is reached, and the other is that the fitness value is no longer updated in several following iterations (i.e., the computation has converged).

(7) Selection, crossover, and mutation processes

The election, crossover, and mutation processes are the fundamental operations for the evolutionary computation of an MA. The proposed MA only performs either the crossover or mutation process. In the selection process, two individuals are randomly selected from the population for the following crossover or mutation operations. In the crossover process, uniform crossover is applied to the proposed MA. When the crossover probability is satisfied, the selected two individuals will be processed by the crossover operation. Figure 6a illustrates the flowchart of the crossover process. In the mutation process, one-point mutation is implemented in the proposed MA. When the mutation probability is satisfied, the selected two individuals will be processed by the mutation operation. Figure 6b illustrates the flowchart of the mutation process.

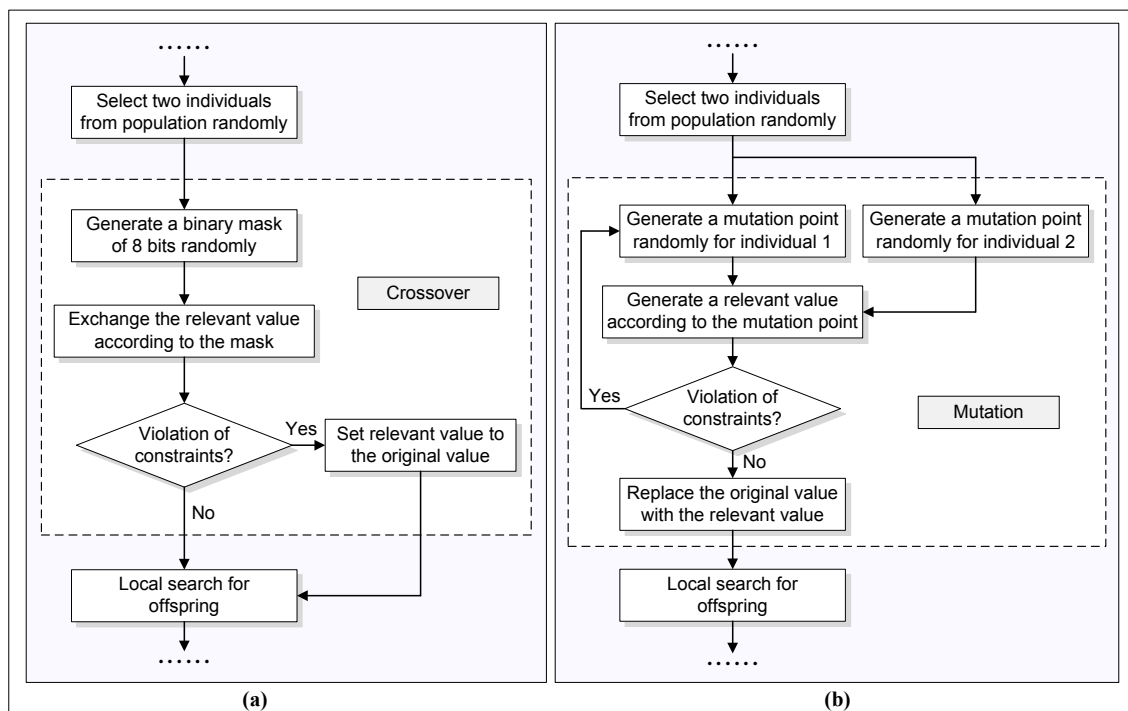


Figure 6. Flowchart for the (a) crossover process; and (b) mutation process.

(8) Replacement process

In order to update the individuals of the population from iteration to iteration, the replacement process is an essential and crucial operation. In the proposed MA, the worst individuals in the population will be replaced with the new individuals. This process is repeated in each next generation until one of the termination conditions is met.

6. Driving Cycles for Optimized Control Strategy of Parallel HEVs

Four different driving cycles, including NEDC, FTP, ECE + EUDC, and UDDS are carried out by the proposed method to find out the optimal control parameters for each driving cycle. The parameters used are listed in Table 4.

The NEDC eliminates the idling period, which causes the engine to start at 0 s, and the emission sampling begins at the same time as the entire cycle [39]. The FTP is used for regulatory emission testing of heavy-duty on-road engines in the United States (40 CFR 86.1333). It is based on the UDDS chassis dynamometer driving cycle and includes “motoring” segments, and therefore, requires a DC or AC electric dynamometer capable of both absorbing and supplying power [40]. The ECE + EUDC is performed on a chassis dynamometer and was used for EU type approval testing of emissions and fuel consumption in light-duty vehicles [EEC Directive 90/C81/01]. This cycle is used for the emission certification of light-duty vehicles in Europe and is also known as the MVEG-A cycle. The entire cycle includes four ECE segments repeated without interruption, followed by one EUDC segment. Before the test, the vehicle is allowed to soak for at least 6 h at a test temperature of 20–30 °C. It is then started and allowed to idle for 40 s [39]. The UDDS is also called FTP-72 (Federal Test Procedure) or LA-4 cycle. It is used for light-duty vehicle testing. The cycle simulates an urban route of 7.5 miles with frequent stops. The maximum speed is 56.7 mph, and the average speed is 19.6 mph. Two phases are included in the cycle: (1) 505 s (3.59 miles at 25.6 mph average speed); and (2) 867 s [41].

Table 4. Parameters for NEDC, FTP, ECE + EUDC, and UDDS driving cycle. NEDC: new European driving cycle; FTP: Federal Test Procedure; ECE + EUDC: Economic Commission for Europe + Extra-Urban driving cycle; UDDS: urban dynamometer driving schedule.

Parameter	Value			
	NEDC	FTP	ECE + EUDC	UDDS
Time	1184 s	2477 s	1225 s	1369 s
Distance	6.79 miles	11.04 miles	6.79 miles	7.45 miles
Maximum speed	74.56 mph	56.70 mph	74.56 mph	56.70 mph
Average speed	20.64 mph	16.04 mph	19.95 mph	19.58 mph
Maximum acceleration	0.00066 mi/s ²	0.00092 mi/s ²	0.00066 mi/s ²	0.00092 mi/s ²
Maximum deceleration	−0.00086 mi/s ²	−0.00092 mi/s ²	−0.00086 mi/s ²	−0.00092 mi/s ²
Average acceleration	0.00034 mi/s ²	0.00034 mi/s ²	0.00034 mi/s ²	0.00031 mi/s ²
Average deceleration	−0.00049 mi/s ²	−0.00036 mi/s ²	−0.00049 mi/s ²	−0.00036 mi/s ²
Idle time	298 s	360 s	339 s	259 s
Number of stops	13	22	13	17
Maximum up grade	0%	0%	0%	0%
Average up grade	0%	0%	0%	0%
Maximum down grade	0%	0%	0%	0%
Average down grade	0%	0%	0%	0%

Data source: ADVISOR, United States Environmental Protection Agency (EPA), and DieselNet.

7. Results

7.1. Parameter Settings

Four parameters are set in the proposed method, i.e., the number of generations, the population size, the probability of crossover, and the probability of mutation. Their values were set to 50, 20, 1.0, and 1.0, respectively. The parameters are chosen by “trial and error.” Furthermore, our experience in algorithmic design has also helped us to select suitable parameters for the problem. The published papers for the algorithms used by the authors can also be referred to [36,37,42–49]. Furthermore, the components for the parallel HEV model are set as shown in Table 5, and the parameters for the used parallel HEV model are set as shown in Table 6.

Table 5. Components for the parallel HEV model.

Component	Version	Type	Description
Vehicle	-	-	Hypothetical small car (VEH_SMCAR)
Fuel Converter	ic	si	Spark Ignition; Geo 1.0 L (41 KW) SI engine (FC_SI41_emis)
Exhaust Aftertreat	-	-	Standard catalyst for stoichiometric SI engine (EX_SI)
Energy Storage	rint	pb	Lead-Acid; Hawker Genesis 12V26Ah10EP VRLA battery, tested by VA Tech. (ESS_PB25)
Motor	-	-	Westinghouse 75-KW (continuous) AC induction motor/inverter (MC_AC75)
Transmission	man	man	Manual transmission; manual 5-speed transmission (TX_5SPD)
Torque Coupling	-	-	Lossless belt drive (TC_DUMMY)
Wheel/Axle	Crr	Crr	Constant coefficient of rolling resistance model; wheel/axle assembly for small car (WH_SMCAR)
Accessory	Const	Const	Constant power accessory load models; 700-W constant electric load (ACC_HYBRID)
Powertrain Control	par	man	Parallel manual transmission; 5-speed parallel charge depleting hybrid (PTC_PAR_CD)
Vehicle	-	-	Hypothetical small car (VEH_SMCAR)
Fuel converter	ic	si	Spark Ignition; Geo 1.0 L (41 KW) SI engine (FC_SI41_emis)

The versions and types are the parameters used in ADVISOR.

Table 6. Parameters for the used parallel HEV model.

Parameter (Unit)	Variable	Value
Mass of the vehicle without components (kg)	veh_glider_mass	592
Cargo mass (kg)	veh_cargo_mass	136
Test mass, including fluids, passengers, and cargo (kg)	veh_mass	1350
Vehicle frontal area (m ²)	veh_FA	2
Coefficient of aerodynamic drag	veh_CD	0.335
Coefficient of wheel rolling resistance	wh_1st_rrc	0.009
Radius of the wheel (m)	wh_radius	0.304

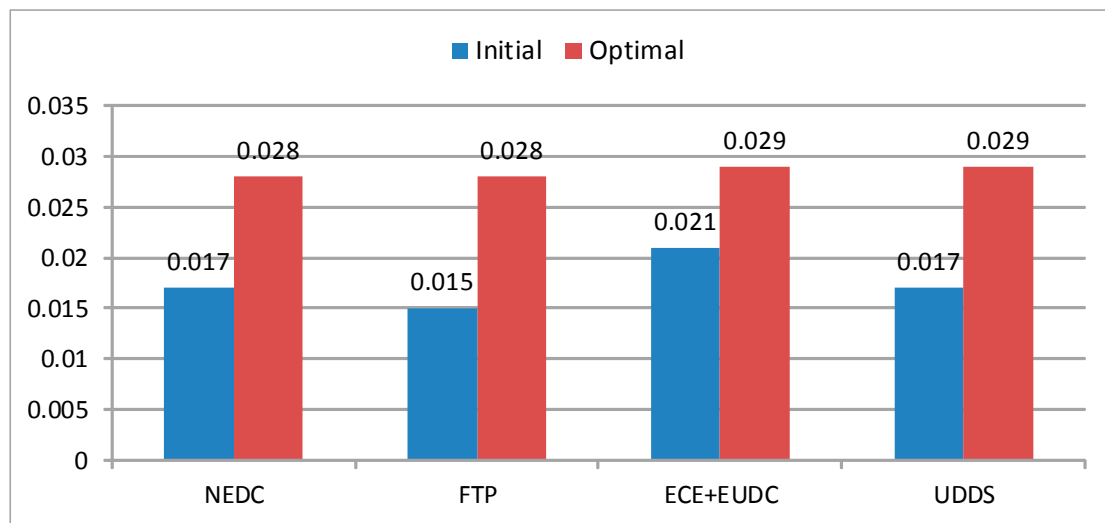
The variables are the parameters used in ADVISOR.

7.2. Results for the Used Driving Cycles

Table 7 shows the initial values and optimal values obtained, and Figure 7 shows the histogram for fitness values obtained using the proposed MA method with the parameters of the control strategy for four driving cycles: NEDC, FTP, ECE + EUDC, and UDDS. The result for the FC and emissions is presented in Table 8 and Figure 8. Further, the result for the dynamic performance is presented in Table 9 and Figure 9. On comparing the results presented in Table 8, Figure 8, Table 9, and Figure 9, we observe that the results obtained using the initial and optimal values of the parameters of the control strategy are very different. The optimal values of the parameters of the control strategy found using the proposed MA method indeed help to reduce the integral FC, HC, CO and NO_x emissions. Furthermore, the dynamic performance not only simultaneously meets the PNGV constraints but also exceeds its requirements. From the above results, the ability of the proposed MA method to optimize the control parameters in parallel HEVs is confirmed. The results used in this study are freely accessible and provided online for those interested [50].

Table 7. The initial values and optimal values of the parameters of the control strategy.

Parameter (Unit)	NEDC		FTP		ECE + EUDC		UDDS	
	Initial	Optimal	Initial	Optimal	Initial	Optimal	Initial	Optimal
SOC_L (-)	0.13	0.276	0.235	0.271	0.306	0.31	0.046	0.267
SOC_H (-)	0.271	0.848	0.433	0.862	0.33	0.931	0.087	0.788
T_{ch} (Nm)	61.144	66.879	74.815	14.61	7.186	14.33	1.41	6.64
T_{min} (-)	0.29	0.211	0.703	0.355	0.83	0.09	0.87	0.798
T_{off} (-)	0.047	0.431	0.891	0.236	0.957	0.084	0.077	0.342
ELS_L (m/s)	12.583	1.998	5.137	2.496	10.974	13.932	4.207	0.23
ELS_H (m/s)	27.902	18.566	25.473	14.75	28.098	25.214	26.695	17.776
D_{ch} (-)	0	1	0	1	1	1	1	1
Fitness value	0.017	0.028	0.015	0.028	0.021	0.029	0.017	0.029

**Figure 7.** The histogram of fitness values for initial and optimal values of the parameters of the control strategy.**Table 8.** The result for fuel consumption (FC) and emissions using initial and optimal values of the parameters of the control strategy.

Parameter (Unit)	NEDC		FTP		ECE + EUDC		UDDS	
	Initial	Optimal	Initial	Optimal	Initial	Optimal	Initial	Optimal
FC (mi/gal)	31.08	31.80	26.69	32.18	32.08	31.72	29.56	29.51
HC (g/mi)	0.71	0.61	0.50	0.47	0.69	0.67	0.63	0.67
CO (g/mi)	8.05	2.93	10.83	3.22	3.73	3.56	5.73	3.81
NO_x (g/mi)	0.68	0.52	0.30	0.45	0.73	0.58	0.65	0.68

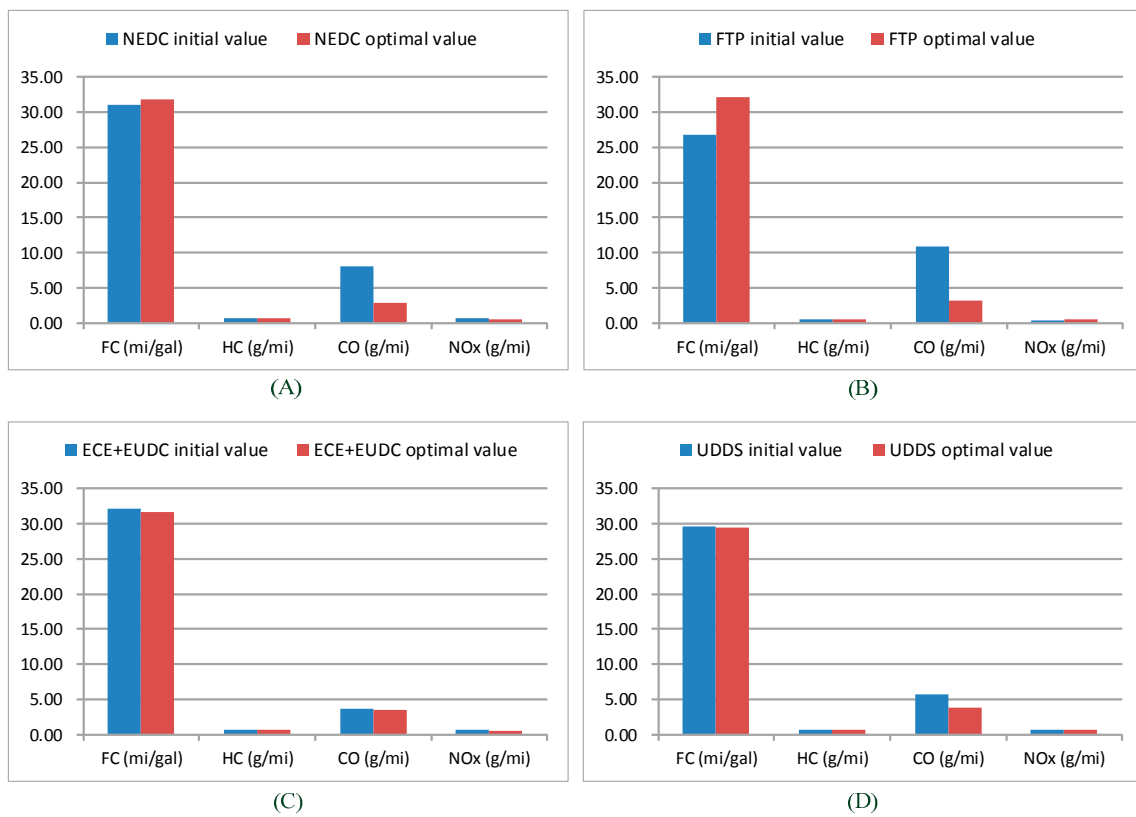


Figure 8. The histogram for FC and emissions using initial and optimal values of the parameters of control strategy. (A) FC and emissions based on NEDC cycle; (B) FC and emissions based on FTP cycle; (C) and emissions based on ECE + EUDC cycle; and (D) FC and emissions based on UDSS cycle.

Table 9. The result for the dynamic performance using initial and optimal values of the parameters of the control strategy.

Parameter (Unit)	NEDC		FTP		ECE + EUDC		UDSS	
	Initial	Optimal	Initial	Optimal	Initial	Optimal	Initial	Optimal
0–60 mph (s)	14.57	9.59	12.67	9.55	12.96	9.18	15.46	9.85
40–60 mph (s)	7.84	4.89	6.81	4.86	6.96	4.61	8.31	5.05
0–85 mph (s)	33.18	19.88	28.36	19.80	29.06	18.76	35.69	20.61
Maximum speed (mi/s)	0.02	0.02	0.02	0.02	0.02	0.02	0.02	0.02
Maximum acceleration (mi/s ²)	0.003	0.003	0.003	0.003	0.003	0.003	0.003	0.003
Distance in 5 s (mi)	0.028	0.034	0.031	0.034	0.030	0.034	0.027	0.033
Gradeability (%)	6.5	6.5	-	6.5	6.5	6.5	-	6.5

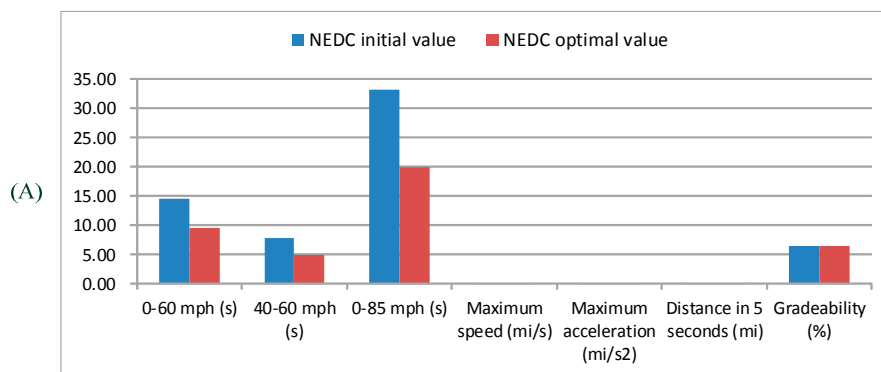


Figure 9. Cont.

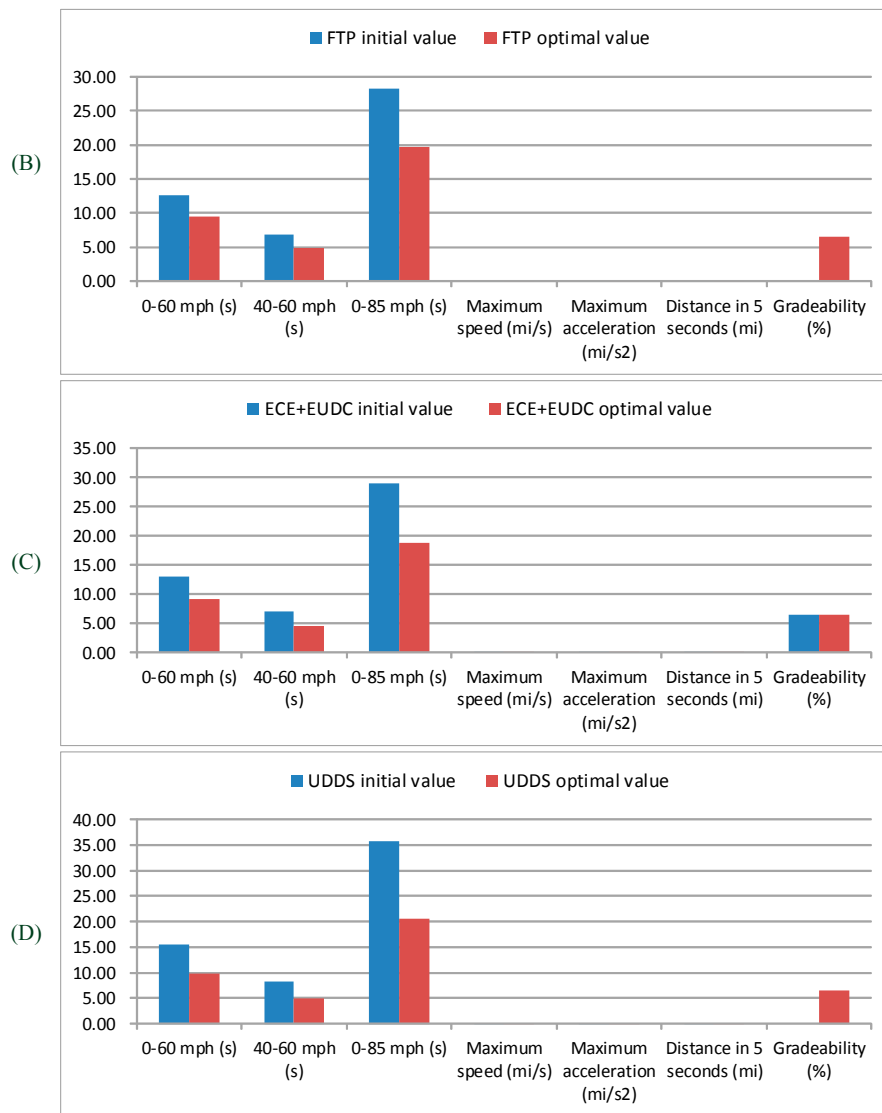


Figure 9. The histogram for dynamic performance using initial and optimal values of the parameters of control strategy. (A) dynamic performance based on NEDC cycle; (B) dynamic performance based on FTP cycle; (C) dynamic performance based on ECE + EUDC cycle; and (D) dynamic performance based on UDSS cycle.

7.3. Analysis of the Results

7.3.1. Improvement in Overall Effectiveness

First, for the observation of the fitness values as shown in Table 7 and Figure 7, the fitness values of the optimal results are 0.011, 0.013, 0.008, and 0.012, which are better than those at the initial conditions in the driving cycles of NEDC, FTP, ECE + EUDC, and UDSS, respectively (as shown in Figure 10). This shows that the proposed MA method is quite useful for selecting a feasible control strategy from the given bounds in the EACS constraints (see Table 3). The improvement in the fitness value means the improvement in overall effectiveness, including the reduction of the FC and emissions, and the improvement or maintain of dynamic performance. Different driving cycles show distinct degrees of improvement owing to the different parameters of each driving cycle (see Table 4).

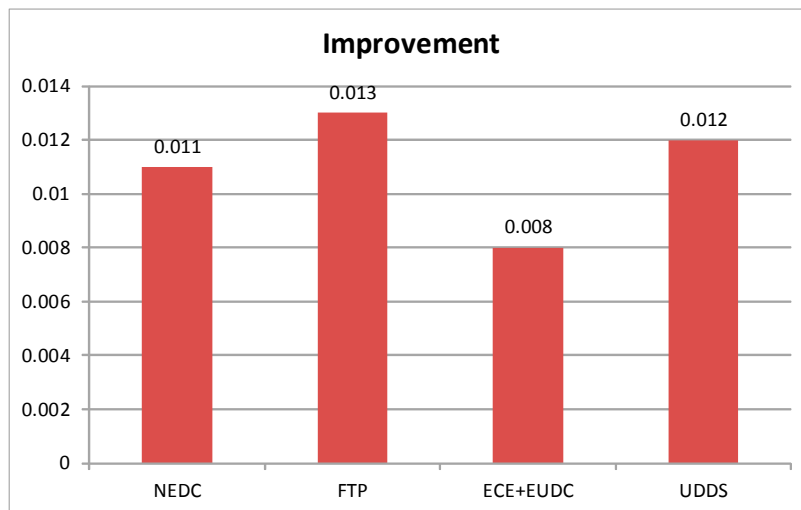


Figure 10. The histogram of the improvement in overall effectiveness between the results using initial and optimal values of the parameters of the control strategy.

7.3.2. Improvement in FC and Emissions

For the FC and emissions (HC, CO, and NO_x) as shown in Table 8 and Figure 8, we observe that the FC is improved for the driving cycles of the NEDC and FTP. The FC is improved by 0.72, 5.49, -0.36, and -0.05 mi/gal for the NEDC, FTP, ECE + EUDC, and UDDS, respectively.

The HC emission is reduced for all the driving cycles except UDDS. The HC emission is reduced by 0.10, 0.03, 0.02, and -0.04 g/mi for the NEDC, FTP, ECE + EUDC, and UDDS, respectively. The CO emission is reduced for all the driving cycles. The CO emission is substantially reduced by 5.12, 7.62, 0.16, and 1.92 g/mi for the NEDC, FTP, ECE + EUDC, and UDDS, respectively. The NO_x emission is improved for the driving cycles of the NEDC and ECE + EUDC. The NO_x emission is reduced by 0.16, -0.15, 0.15, and -0.03 g/mi for the NEDC, FTP, ECE + EUDC, and UDDS, respectively. The improvement results for the FC and emissions are shown in Figure 11. Although some values of the parameters are not greatly improved, their improved values are reflected in the other parameters or the following resultant dynamic performance.

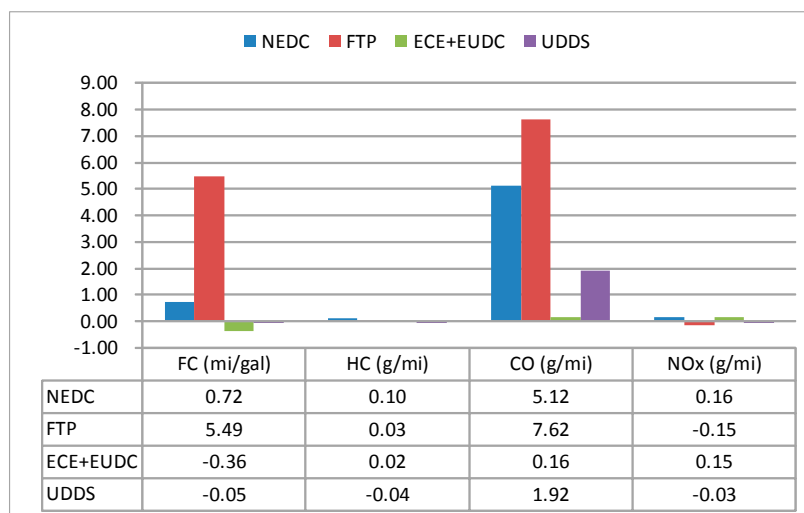


Figure 11. The histogram of the improvements in FC and emissions between the results using initial and optimal values of the parameters of control strategy.

7.3.3. Improvement in Dynamic Performance

With respect to the dynamic performance, all the optimal values of the control strategy satisfy the seven PNGV dynamic performance constraints and the dynamic performance shows improvements from the initial conditions as shown in Table 2. Table 9 and Figure 9 show the improved results. The improvement in the dynamic performance is shown in Figure 10. For the NEDC, the acceleration time is reduced by 4.98, 2.96, and 13.29 s for 0–60 mph, 40–60 mph, and 0–85 mph, respectively. The maximum speed is increased by 0.003 mi/s, the maximum acceleration is maintained at the original value of 0.003 mi/s², the distance traveled in 5 s is increased by 0.005 mi, and the gradeability is maintained at 6.5%. For the FTP, the acceleration time is reduced by 3.12, 1.94, and 8.56 s for 0–60 mph, 40–60 mph, and 0–85 mph, respectively. The maximum speed is increased by 0.002 mi/s, the maximum acceleration is maintained at the original value of 0.003 mi/s², the distance traveled in 5 s is increased by 0.003 mi, and the gradeability increased from 0% to 6.5%. For the ECE + EUDC, the acceleration time is reduced by 3.79, 2.35, and 10.31 s for 0–60 mph, 40–60 mph, and 0–85 mph, respectively. The maximum speed is increased by 0.003 mi/s, the maximum acceleration is maintained at its original value of 0.003 mi/s², the distance traveled in 5 s is increased by 0.004 mi, and the gradeability is maintained at the original value of 6.5%. Finally, for the UDDS, the acceleration time is reduced by 5.61, 3.27, and 15.08 s for 0–60 mph, 40–60 mph, and 0–85 mph, respectively. The maximum speed is increased in 0.003 mi/s, the maximum acceleration is maintained at its original value of 0.003 mi/s², the distance traveled in 5 s is increased by 0.006 mi, and the gradeability improves from 0% to 6.5%. These improvements in the dynamic performance are shown in Figure 12.

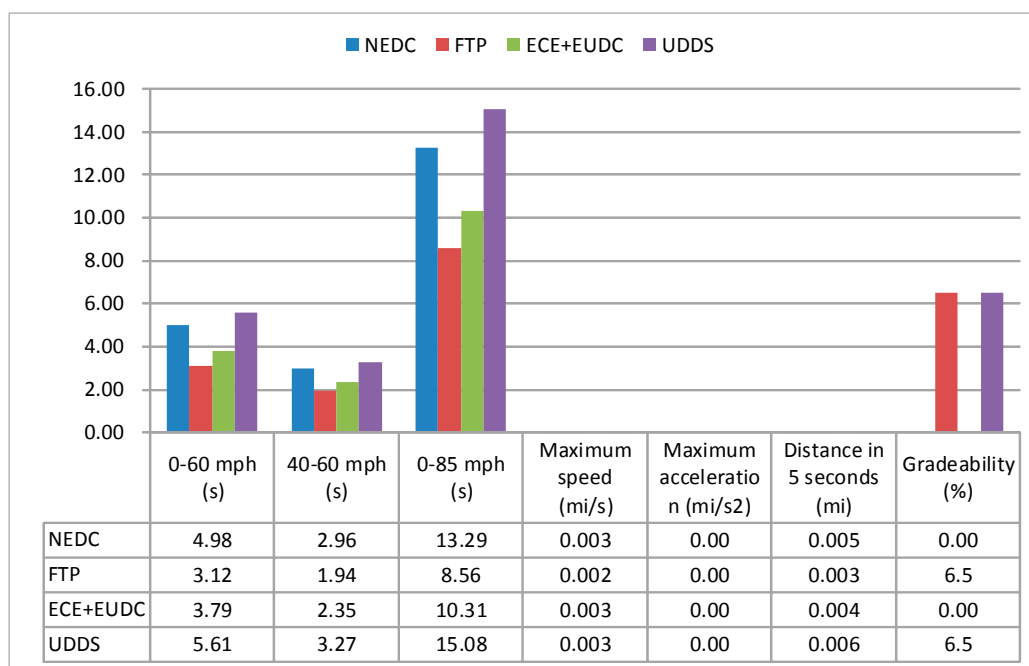


Figure 12. The histogram of the improvements in the dynamic performance between the results using initial and optimal values of the parameters of the control strategy.

8. Conclusions

This study proposes a robust evolutionary computation method called a “memetic algorithm (MA)” to optimize the control parameters in parallel HEVs. Its “local search” mechanism greatly enhances the search capabilities for obtaining optimal values of the parameters of the control strategy. We combine the ADVISOR with the fitness function in the proposed MA method and use it to effectively evaluate the FC and emissions (HC, CO, and NO_x) of the vehicle engine based on the

EACS. Furthermore, we consider that the driving performance requirements, which are referred to as the PNGV constraints, must be satisfied simultaneously. In order to verify the proposed method, we have employed four different driving cycles—NEDC, FTP, ECE + EUDC, and UDDS; the results for these driving cycles are verified. The fitness values of the optimal results are 0.011, 0.013, 0.008, and 0.012, which are better than those of the initial conditions in the driving cycles of the NEDC, FTP, ECE + EUDC, and UDDS, respectively. For the FC and emissions (HC, CO, and NO_x), the FC is improved by 0.72 and 5.49 mi/gal for the NEDC and FTP, respectively. The HC emission is reduced by 0.10, 0.03, and 0.02 g/mi for the NEDC, FTP, and ECE + EUDC, respectively. The CO emission is substantially reduced by 5.12, 7.62, 0.16, and 1.92 g/mi for the NEDC, FTP, ECE + EUDC, and UDDS, respectively. The NO_x emission is a reduced by 0.16 and 0.15 g/mi for the NEDC and ECE + EUDC, respectively. With regard to the dynamic performance, all the optimal values of the control strategy satisfy the seven PNGV dynamic performance constraints. The acceleration time is reduced by 4.98, 2.96, and 13.29 s for 0–60 mph, 40–60 mph, and 0–85 mph, respectively; the maximum speed is increased by 0.003 mi/s; and the distance traveled in 5 s is increased by 0.005 mi for the NEDC. The acceleration time is respectively reduced in 3.12, 1.94, and 8.56 s for 0–60 mph, 40–60 mph, and 0–85 mph; the maximum speed is increased in 0.002 mi/s; the distance traveled in 5 s is increased in 0.003 mi for the FTP. The acceleration time is reduced by 3.79, 2.35, and 10.31 s for 0–60 mph, 40–60 mph, and 0–85 mph, respectively; the maximum speed is increased by 0.003 mi/s; and the distance traveled in 5 s is increased by 0.004 mi for the ECE + EUDC. The acceleration time is reduced by 5.61, 3.27, and 15.08 s for 0–60 mph, 40–60 mph, and 0–85 mph, respectively; the maximum speed is increased by 0.003 mi/s; and the distance traveled in 5 s is increased by 0.006 mi for the UDDS. Furthermore, the maximum acceleration is maintained at 0.003 mi/s² and the gradeability reached a value of 6.5% in all the considered driving cycles. The results indicate that the proposed MA method is capable of determining the optimal parameters of the control strategy for parallel HEVs. It helps to improve the fuel consumption and reduce the emissions, as well as guarantee vehicle performance.

Acknowledgments: This work is partly supported by the Ministry of Science and Technology (MOST) in Taiwan under grant MOST105-2221-E-324-026, MOST105-2221-E-027-096, and MOST106-3113-E-027-008.

Author Contributions: Yu-Huei Cheng substantially contributed to the algorithm design, the development of the algorithm, production and analysis of the results, and preparation of the manuscript for this study. Ching-Ming Lai substantially contributed to the examination and interpretation of the results, and the review and proofreading of the manuscript.

Conflicts of Interest: The authors declare no conflict of interest.

Abbreviation

Acronym	Term	Description
ADVISOR	advanced vehicle simulator	A simulator for vehicles uses MATLAB/Simulink.
BA	bees algorithm	An evolutionary computation method that based on bees foraging.
BCS	baseline control strategy	A point of reference for control strategy in vehicles.
CO	carbon monoxide	The exhaust gas from vehicles.
DP	dynamic programming	An algorithmic method that applies solutions to larger and larger cases to inductively solve a computational problem for a given instance.
EACS	electric assist control strategy	A rule-based strategy for power distribution between power sources.
ECE + EUDC	Economic Commission for Europe + Extra-Urban Driving Cycle	A driving cycle.
EM	electric motor	An electric motor is a machine that converts electrical energy into mechanical energy.

Acronym	Term	Description
FTP	Federal Test Procedure	A driving cycle is used for regulatory emission testing of heavy-duty on-road engines in the United States.
GA	genetic algorithm	An evolutionary computation method inspired by the mechanisms of genetics.
HC	hydrocarbons	The exhaust gas from vehicles.
HEV	hybrid electric vehicle	HEVs have both a petrol- or diesel-powered combustion engine and an electric engine.
ICE	internal combustion engine	An engine of one or more working cylinders in which the process of combustion takes place within the cylinders.
MA	memetic algorithm	An evolutionary computation method inspired by Dawkins' notion of a meme. MA is similar to GA yet superior to GA. The mechanism of local search is one of its main features.
NEDC	new European driving cycle	A driving cycle eliminates the idling period that makes engine starts at 0s and the emission sampling begins at the same time as the entire cycle.
NO _x	nitrogen oxides	The exhaust gas from vehicles.
PMP	Pontryagin's minimum principle	The principle is used in optimal control theory to find the best possible control for taking a dynamical system from one state to another, especially in the presence of constraints for the state or input controls.
PNGV	Partnership for a New Generation of Vehicles	A cooperative research program between the U.S. government and major auto corporations, aimed at bringing extremely fuel-efficient (up to 80 mpg) vehicles to market by 2003.
PSO	particle swarm optimization	An evolutionary computation method based on swarm behavior of animals, like bird flocking.
SOC	state of charge	The equivalent of a fuel gauge for the battery pack in a battery electric vehicle (BEV), hybrid vehicle (HV), or plug-in hybrid electric vehicle (PHEV).
UDDS	Urban Dynamometer Driving Schedule	A driving cycle used for light duty vehicle testing. It simulates an urban route of 7.5 mile with frequent stops.

References

- Gao, Y.; Rahman, K.M.; Ehsani, M. Parametric design of the drive train of an electrically peaking hybrid (ELPH) vehicle. *SAE Tech. Pap.* **1997**. [[CrossRef](#)]
- Tanoue, K.; Yanagihara, H.; Kusumi, H. Hybrid is a key technology for future automobiles. In *Hydrogen Technology*; Springer: New York, NY, USA, 2008; pp. 235–272.
- Baumann, B.M.; Washington, G.; Glenn, B.C.; Rizzoni, G. Mechatronic design and control of hybrid electric vehicles. *IEEE/ASME Trans. Mechatron.* **2000**, *5*, 58–72. [[CrossRef](#)]
- Johnson, V.H.; Wipke, K.B.; Rausen, D.J. HEV control strategy for real-time optimization of fuel economy and emissions. *SAE Trans.* **2000**, *109*, 1677–1690.
- Pisu, P.; Rizzoni, G. A comparative study of supervisory control strategies for hybrid electric vehicles. *IEEE Trans. Control Syst. Technol.* **2007**, *15*, 506–518. [[CrossRef](#)]
- Salmasi, F.R. Control strategies for hybrid electric vehicles: Evolution, classification, comparison, and future trends. *IEEE Trans. Veh. Technol.* **2007**, *56*, 2393–2404. [[CrossRef](#)]
- Barambones, O. Sliding mode control strategy for wind turbine power maximization. *Energies* **2012**, *5*, 2310–2330. [[CrossRef](#)]

8. Zou, Y.; Sun, F.; Hu, X.; Guzzella, L.; Peng, H. Combined optimal sizing and control for a hybrid tracked vehicle. *Energies* **2012**, *5*, 4697–4710. [[CrossRef](#)]
9. Guo, H.; He, H.; Sun, F. A combined cooperative braking model with a predictive control strategy in an electric vehicle. *Energies* **2013**, *6*, 6455–6475. [[CrossRef](#)]
10. Zou, Y.; Hou, S.-J.; Li, D.-G.; Wei, G.; Hu, X.-S. Optimal energy control strategy design for a hybrid electric vehicle. *Discret. Dyn. Nat. Soc.* **2013**, *2013*, 132064. [[CrossRef](#)]
11. Yu, H.; Kuang, M.; McGee, R. Trip-oriented energy management control strategy for plug-in hybrid electric vehicles. *IEEE Trans. Control Syst. Technol.* **2014**, *22*, 1323–1336.
12. Lin, C.-C.; Peng, H.; Grizzle, J.W.; Kang, J.-M. Power management strategy for a parallel hybrid electric truck. *IEEE Trans. Control Syst. Technol.* **2003**, *11*, 839–849.
13. Kim, N.; Cha, S.; Peng, H. Optimal control of hybrid electric vehicles based on Pontryagin’s minimum principle. *IEEE Trans. Control Syst. Technol.* **2011**, *19*, 1279–1287.
14. Assanis, D.; Delagrammatikas, G.; Fellini, R.; Filipi, Z.; Liedtke, J.; Michelena, N.; Papalambros, P.; Reyes, D.; Rosenbaum, D.; Sales, A. Optimization approach to hybrid electric propulsion system design. *J. Struct. Mech.* **1999**, *27*, 393–421. [[CrossRef](#)]
15. Sciarretta, A.; Back, M.; Guzzella, L. Optimal control of parallel hybrid electric vehicles. *IEEE Trans. Control Syst. Technol.* **2004**, *12*, 352–363. [[CrossRef](#)]
16. Johri, R.; Filipi, Z. Self-learning neural controller for hybrid power management using neuro-dynamic programming. *SAE Tech. Pap.* **2011**. [[CrossRef](#)]
17. Poursamad, A.; Montazeri, M. Design of genetic-fuzzy control strategy for parallel hybrid electric vehicles. *Control Eng. Pract.* **2008**, *16*, 861–873. [[CrossRef](#)]
18. Panday, A.; Bansal, H.O. Energy management strategy implementation for hybrid electric vehicles using genetic algorithm tuned Pontryagin’s minimum principle controller. *Int. J. Veh. Technol.* **2016**, *2016*, 4234261. [[CrossRef](#)]
19. Montazeri-Gh, M.; Poursamad, A.; Ghalichi, B. Application of genetic algorithm for optimization of control strategy in parallel hybrid electric vehicles. *J. Frankl. Inst.* **2006**, *343*, 420–435. [[CrossRef](#)]
20. Moore, T.C.; Lovins, A.B. Vehicle design strategies to meet and exceed PNGV goals. *SAE Tech. Pap.* **1995**. [[CrossRef](#)]
21. Wu, J.; Zhang, C.-H.; Cui, N.-X. PSO algorithm-based parameter optimization for HEV powertrain and its control strategy. *Int. J. Automot. Technol.* **2008**, *9*, 53–59. [[CrossRef](#)]
22. Long, V.; Nhan, N. Bees-algorithm-based optimization of component size and control strategy parameters for parallel hybrid electric vehicles. *Int. J. Automot. Technol.* **2012**, *13*, 1177–1183. [[CrossRef](#)]
23. Hao, J.; Yu, Z.; Zhao, Z.; Shen, P.; Zhan, X. Optimization of key parameters of energy management strategy for hybrid electric vehicle using DIRECT algorithm. *Energies* **2016**, *9*, 997. [[CrossRef](#)]
24. Sciarretta, A.; Guzzella, L. Control of hybrid electric vehicles. *IEEE Control Syst.* **2007**, *27*, 60–70. [[CrossRef](#)]
25. Malikopoulos, A.A. Supervisory power management control algorithms for hybrid electric vehicles: A survey. *IEEE Trans. Intell. Transp. Syst.* **2014**, *15*, 1869–1885. [[CrossRef](#)]
26. Moscato, P. On evolution, search, optimization, genetic algorithms and martial arts: Towards memetic algorithms. In *Caltech Concurrent Computation Program; C3P Report*; California Institute of Technology: Pasadena, CA, USA, 1989.
27. Dawkins, R. *The Selfish Gene*; Oxford University Press: Oxford, UK, 2016.
28. Merz, P.; Freisleben, B. A genetic local search approach to the quadratic assignment problem. In Proceedings of the 7th International Conference on Genetic Algorithms, East Lansing, MI, USA, 19–23 July 1997.
29. Matthé, R.; Eberle, U. *The Voltec System: Energy Storage and Electric Propulsion*; Elsevier: Amsterdam, The Netherlands, 2014; pp. 151–176.
30. Chau, K.; Wong, Y. Overview of power management in hybrid electric vehicles. *Energy Convers. Manag.* **2002**, *43*, 1953–1968. [[CrossRef](#)]
31. Hermance, D.; Sasaki, S. Hybrid electric vehicles take to the streets. *IEEE Spectr.* **1998**, *35*, 48–52. [[CrossRef](#)]
32. Yamaguchi, J. Insight by Honda. *Automot. Eng. Int.* **1999**, *107*, 55–57.
33. Sawaragi, Y.; Nakayama, H.; Tanino, T. *Theory of Multiobjective Optimization*; Elsevier: Amsterdam, The Netherlands, 1985; Volume 176.
34. Martorell, S.; Carlos, S.; Sanchez, A.; Serradell, V. Constrained optimization of test intervals using a steady-state genetic algorithm. *Reliab. Eng. Syst. Saf.* **2000**, *67*, 215–232. [[CrossRef](#)]

35. Yeniay, Ö. Penalty function methods for constrained optimization with genetic algorithms. *Math. Comput. Appl.* **2005**, *10*, 45–56. [[CrossRef](#)]
36. Yang, C.H.; Cheng, Y.H.; Chuang, L.Y.; Chang, H.W. Specific PCR product primer design using memetic algorithm. *Biotechnol. Progress* **2009**, *25*, 745–753. [[CrossRef](#)] [[PubMed](#)]
37. Chuang, L.-Y.; Cheng, Y.-H.; Yang, C.-H. PCR-CTPP design for enzyme-free SNP genotyping using memetic algorithm. *IEEE Trans. Nanobiosci.* **2015**, *14*, 13–23. [[CrossRef](#)] [[PubMed](#)]
38. Markel, T.; Brooker, A.; Hendricks, T.; Johnson, V.; Kelly, K.; Kramer, B.; O’Keefe, M.; Sprik, S.; Wipke, K. ADVISOR: A systems analysis tool for advanced vehicle modeling. *J. Power Sources* **2002**, *110*, 255–266. [[CrossRef](#)]
39. ECE 15 + EUDC/NEDC. Available online: https://www.dieselnet.com/standards/cycles/ece_eudc.php (accessed on 14 January 2017).
40. Heavy-Duty FTP Transient Cycle. Available online: https://www.dieselnet.com/standards/cycles/ftp_trans.php (accessed on 14 January 2017).
41. FTP-72 (UDDS). Available online: <https://www.dieselnet.com/standards/cycles/ftp72.php> (accessed on 14 January 2017).
42. Yang, C.-H.; Cheng, Y.-H.; Chuang, L.-Y. PCR-CTPP design based on particle swarm optimization with fuzzy adaptive strategy. *Eng. Lett.* **2012**, *20*, 196–202.
43. Cheng, Y.-H.; Chuang, L.-Y.; Yang, C.-H. Single nucleotide polymorphisms polymerase chain reaction-restriction fragment length polymorphism primer design using genetic algorithm with fixed and adaptive stopping criteria. *J. Adv. Math. Appl.* **2013**, *2*, 172–181. [[CrossRef](#)]
44. Chuang, L.-Y.; Cheng, Y.-H.; Yang, C.-H.; Yang, C.-H. Associate PCR-RFLP assay design with SNPs based on genetic algorithm in appropriate parameters estimation. *IEEE Trans. Nanobiosci.* **2013**, *12*, 119–127. [[CrossRef](#)] [[PubMed](#)]
45. Cheng, Y.-H. Computational intelligence-based polymerase chain reaction primer selection based on a novel teaching-learning-based optimisation. *IET Nanobiotechnol.* **2014**, *8*, 238–246. [[CrossRef](#)] [[PubMed](#)]
46. Cheng, Y.-H. Estimation of teaching-learning-based optimization primer design using regression analysis for different melting temperature calculations. *IEEE Trans. Nanobiosci.* **2015**, *14*, 3–12. [[CrossRef](#)] [[PubMed](#)]
47. Cheng, Y.-H. A novel teaching-learning-based optimization for improved mutagenic primer design in mismatch PCR-RFLP SNP genotyping. *IEEE/ACM Trans. Comput. Biol. Bioinform.* **2016**, *13*, 86–98. [[CrossRef](#)] [[PubMed](#)]
48. Cheng, Y.-H.; Kuo, C.-N.; Lai, C.-M. Effective natural PCR-RFLP primer design for SNP genotyping using teaching-learning-based optimization with elite strategy. *IEEE Trans. Nanobiosci.* **2016**, *15*, 657–665. [[CrossRef](#)] [[PubMed](#)]
49. Cheng, Y.-H.; Kuo, C.-N.; Lai, C.-M. An improved evolutionary method with test in different crossover rates for PCR-RFLP SNP genotyping primer design. *Int. J. Min. Metall. Mech. Eng.* **2016**, *4*, 25–29.
50. The results for CSMA. Available online: <https://sites.google.com/site/yhcheng1981/csma> (accessed on 14 January 2017).

